Astron. Astrophys. 93, 178–188 (1981)

ASTRONOMY AND ASTROPHYSICS

Theoretical Stellar Chromospheres of Late Type Stars

V. Temperature Minimum in the Grey LTE Approach

F. Schmitz and P. Ulmschneider

Institut für Astronomie und Astrophysik der Universität Würzburg, Am Hubland, D-8700 Würzburg, Federal Republic of Germany

Received February 13, accepted May 19, 1980

Summary. With the computation of theoretical chromosphere models for a number of stars with $T_{\rm eff}=4000$ to 7000 K and $\log g=2$ to 5 the monochromatic, grey LTE radiation hydrodynamic approach of the acoustic heating theory is brought to its conclusion. We compare our theoretical predictions with observations and find rather good agreement for the position of the temperature minima, the total chromospheric radiation flux as well as the average $T_{\rm eff}$ slope of the Mg II emission. Both theoretical and observed stellar chromospheres fall into two classes denoted *S*- and *R*-types. Empirically found temperature enhancement is proposed to be due to the large acoustic wave amplitude and the non-linearity of the Planck function. The shortcomings of the acoustic heating theory are extensively discussed.

Key words: acoustic heating – theoretical chromosphere models – chromospheric emission

1. Introduction

In this series of papers we construct one dimensional theoretical models of stellar chromospheres based on the short period acoustic heating theory and compare these models with observations. The acoustic heating theory has first been proposed by Biermann (1946) and assumes that the chromospheric layers of a star are heated by acoustic shock waves. These develop out of acoustic waves which in turn are generated in the convection zone of the star. Attempting a fully theoretical approach for a star of given effective temperature $T_{\rm eff}$ and gravity g, we start with the computation of a convection zone model employing a stellar envelope code which is based on the mixing length theory of Böhm-Vitense (1958). In this theory the parameter α, the ratio of mixing length and pressure scale height has to be specified. On basis of the convection zone model the acoustic energy generation is computed using the Lighthill (1952, 1954) – Proudman (1952) theory. With the acoustic flux spectrum presently replaced by a delta function, solving the hydrodynamic equations and the radiative transfer equation in the grey approximation we compute the propagation of the acoustic waves, the formation of shock waves and the radiative and mechanical energy balance in the outer stellar atmosphere. From time averaged results we derive one dimensional theoretical chromosphere models which are then compared with semi-empirical models. This purely theoretical approach has the disadvantage that errors encountered at each of the three principal steps accumulate. In a comparison with observations this has to be kept in mind when reasons for discrepancies are investigated. A fully theoretical approach however has the advantage that the feasibility of an acoustically heated chromosphere may be demonstrated and that general trends in the properties of theoretical stellar chromospheres can be derived and compared with observations.

The state of this approach at the present time can be summarized as follows. The computations of convection zone models and the calculation of the acoustic energy generation for a large sample of late type stars is described in Paper I (Renzini et al., 1977). In Paper II (Ulmschneider et al., 1977b) we have computed the shock formation of the acoustic waves for a smaller group of stars. Comparing shock formation heights with semi-empirical temperature minimum heights we detected considerable discrepancies (Cram and Ulmschneider, 1978). Similar disparities have been reported by Linsky and Ayres (1978) in a comparison of observed Mg II h and k line fluxes with theoretical acoustic energy fluxes at the height of shock formation given by Paper II.

In a detailed analysis of the development and dissipation of acoustic shock waves for Arcturus (Ulmschneider et al., 1979) it was realized that one reason for the considerable discrepancy between theory and observation for this star was that the theoretical temperature minimum height cannot always be identified with the shock formation height. As discussed below the identification of temperature minimum positions with shock heights is only true for stars with an *S*-type chromosphere (this term is defined in Sect. 3a). In Arcturus which has an *R*-type chromosphere (cf. Sect. 3a) shock formation occurs in the radiative damping zone which slows further growth of the acoustic wave. Only after the damping zone is passed does the wave amplitude and with it the dissipation grow rapidly enough that a temperature minimum is formed. For Arcturus this effect produces a considerable height distance between the point of shock formation and the position of the temperature minimum.

In Papers III and IV (Schmitz and Ulmschneider, 1980a, b) detailed comparisons between theoretical and semi-empirical temperature minimum heights as well as between acoustic fluxes and semi-empirical chromospheric radiation loss rates were made for nine additional late type giant and dwarf stars. It was found that for most stars the agreement between theory and observation in view of the possible errors appears surprisingly good. Only for late type dwarf stars do we have a considerable discrepancy. This discrepancy has already been noted by Blanco et al. (1974).

As shown in Papers III and IV this remaining discrepancy would be removed if more acoustic energy were available. Presently however an improved method for the computation of

Send offprint request to: P. Ulmschneider

the acoustic energy production is explored by Bohn (1980). In preliminary results Bohn has found for late type dwarfs enhancements of the acoustic flux by several orders of magnitude.

However active chromosphere stars like EQ Vir discussed in Paper IV as well as RS CVn binaries like HR 1099 and UX Ari observed by Basri and Linsky (1979) may well show the limit of the acoustic approach. If enhancement of the acoustic energy generation by the magnetic fields in these stars proves insufficient we will be forced to search for an additional presently unknown magnetic heating mechanism to supplement or even replace the acoustic process.

In the present work our approach using a grey LTE radiation hydrodynamic approximation for the acoustic wave propagation is brought to its conclusion. For late type stars with $T_{\rm eff}=4000$ K to 8000 K and $\log g=1$ to 5 we compute theoretical chromosphere models, and predict temperature minima as well as chromospheric emission fluxes. The method of computation is the same as described in Papers III and IV with the following exceptions. In all models we have assumed a common value of $\alpha=1.25$ and have taken the opacity table of Kurucz (1979). The value of α has been chosen for ease of comparison with our previous work and to reduce the sharply increased computer time necessary when the opacity table is used instead of the simple opacity law. This value is rather low compared to the values of $\alpha\simeq 2.0$ found by Ulrich and Rhodes (1977) as well as Rhodes et al. (1977) in a comparison between computed and observed envelope eigenfrequencies of the sun. However low horizontal wave number eigenmode observations of Claverie et al. (1979) agree best with models of Iben and Mahaffy (1976) using $\alpha<0.6$ and with a model of Christensen-Dalsgaard et al. (1979) using $\alpha=1.11$. Both of these models have low heavy element abundances. Nevertheless using the $\alpha^{2.8}$ dependence of the acoustic flux generation as found in Paper I and the discussion of the α-dependence of the temperature minimum heigts and acoustic fluxes as given in Paper III our present results can be modified for other values of α.

The second modification is that for our initial models we now take convection into account in order to considerably reduce the steep temperature gradient encountered in purely radiative models of stars of higher $T_{\rm eff}$. These modifications are discussed in Sect. 2. The results are exhibited in Sect. 3 while Sect. 4 gives a discussion followed by conclusions.

2. Method

a) Energy Generation

Our method to compute a convection zone model and the acoustic energy generation with the Lighthill-Proudman theory has been described in Paper I and will not be repeated here. As discussed in Paper III the acoustic flux of Paper I has to be multiplied by a factor of two to account for the reflection of the inward going energy. Figure 1 shows the newly computed acoustic flux F_{Mo} for the case that the ratio of the mixing length to the pressure scale height is $\alpha=1.25$. The method described in Paper I does not allow to compute the acoustic flux spectrum. However more refined calculations of Stein (1968, 1970) and Bohn (1980) show that the maximum of the acoustic flux spectrum is roughly at the period

$$P_{\max}\simeq\frac{1}{10}P_A=\frac{1}{10}\,\frac{4\pi c}{\gamma g}\simeq\frac{H}{c}\,. \qquad (1)$$

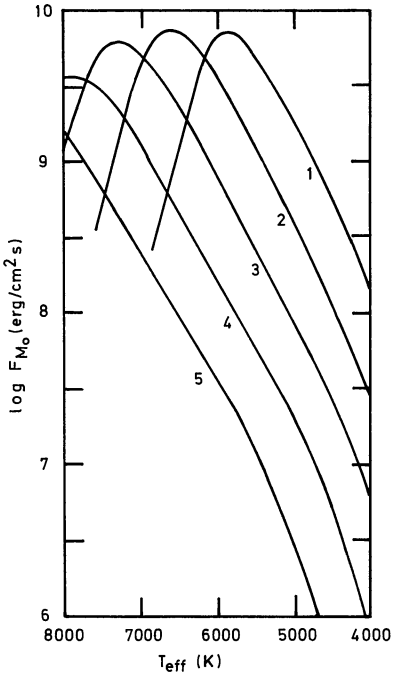

Fig. 1. Acoustic energy fluxes F_{Mo} as function of the effective temperature $T_{\rm eff}$ with the logarithm of the gravity g as parameter based on the Lighthill-Proudman theory ($\alpha=1.25$, $X=0.7$, and $Z=0.02$)

Here P_A is the acoustic cut off period, c the sound velocity, H the pressure scale height and γ the ratio of specific heats. These values were taken at the point of maximum acoustic energy generation. Table 1 gives the period $P=P_{\max}$ computed using Eq. (1). In our present approach we replace the acoustic frequency spectrum by a delta function at the period $P=P_{\rm Max}$.

b) Ambient Atmosphere Models with Convection

In previous work we have initially used a perturbation approach (Paper II) where the acoustic waves propagate on a prescribed ambient model atmosphere for which we have taken the non-grey radiative and convective equilibrium models of Carbon and Gingerich (1969) as well as Kurucz (1979). Our more recent approach (Papers III, IV) uses grey radiative equilibrium models as initial atmospheres. Both approaches satisfy the requirement that in absence of a wave disturbance the initial atmosphere does not show any secular changes in a time-dependent hydrodynamic calculation. In the perturbation approach this was achieved by modifying the energy equation and considering only terms proportional to the wave disturbance. Alternatively in the grey approach the proper choice of the initial atmosphere model ensured the time independence for the grey radiation hydrodynamic code. However it is well known that radiative equilibrium models give a rather poor representation of the deeper layers of stellar photosphere, especially for stars with higher $T_{\rm eff}$. Here our grey radiative equilibrium models had unrealistically steep temperature gradients which led to numerical difficulties when the acoustic waves entered the lower boundary. In order to avoid these difficulties and to model a more realistic situation we now include convection. Time independence of the initial atmosphere was ensured by the use of grey radiative and convective equilibrium models which we constructed according to the method

Table 1. Summary of physical variables for theoretical stellar chromosphere models of given effective temperature $T_{\rm eff}$ and gravity g. P is the acoustic period, F_{MO} the initial acoustic flux, $\tau_{1/2}$ the optical depth where one half of the initial acoustic flux has been generated, F_{MS} the acoustic flux at shock formation, F_{MT} the acoustic flux at the temperature minimum, m_L height of the outer limit of the radiative damping zone, m_S the height of shock formation, m_T the height of the temperature minimum, T_T the minimum temperature and T_{RE} the radiative equilibrium boundary temperature. Heights m are measured in terms of mass column density

$T_{\rm eff}$	(K)	4000	4000	4000	4500	4500	5000	5000	6000	6000	7000
$\log g$	(cm s^{-2})	2	3	4	2	3	3	4	4	5	5
P	(s)	7.4E3	6.7E2	5.8E1	7.8E3	7.3E2	7.8E2	7.2E1	8.4E1	7.7E0	9.0E0
F_{MO}	(erg cm^{-2} s^{-1})	3.0E7	6.4E6	6.8E5	1.1E8	2.7E7	8.6E7	2.0E7	1.6E8	3.6E7	2.2E8
$\tau_{1/2}$		80	60	10	70	50	50	40	30	20	40
F_{MS}	(erg cm^{-2} s^{-1})	1.2E7	1.4E6	2.2E5	7.2E7	3.7E6	3.5E7	2.0E6	3.5E7	5.0E6	5.0E7
F_{MT}	(erg cm^{-2} s^{-1})	4.5E6	1.2E6	2.0E5	9.0E6	3.2E6	1.0E7	1.7E6	1.5E7	4.0E6	3.5E7
m_L	(g cm^{-2})	1.7E1	2.7E1	1.8E1	1.8E0	6.3E0	1.4E0	2.9E0	7.5E−1	1.0E0	3.1E−1
m_S	(g cm^{-2})	2E1	2E−1	4E−3	4E1	5E−1	6E0	3E−2	7E−1	7E−3	5E−2
m_T	(g cm^{-2})	2.4E0	1.3E−1	2.5E−3	3.25E0	3.1E−1	1.0E0	2.0E−2	1.5E−1	4.0E−3	2.3E−2
T_T	(K)	3010	3120	3177	3310	3470	3850	3950	4670	4750	5330
T_{RE}	(K)	3245	3245	3245	3650	3650	4056	4056	4867	4867	5678

described by Kurucz (1973) for his ATLAS code. The temperature correction procedure was modified to allow for our grey two stream radiation treatment which uses the opacity table of Kurucz (1979) with normal metal abundance.

c) Time-dependent Calculations with Convection

As it is impossible in a one-dimensional calculation to include time-dependent convection we assume that the convective energy transport remains at its steady state value in our calculations. That is, in our hydrodynamic computation only the radiative and acoustic energy transport will show time dependence. The energy equation (cf. Ulmschneider et al., 1977a; Kalkofen and Ulmschneider, 1977) is now modified to read

$$T\left(\frac{\partial S}{\partial t}\right)_a = T\left.\frac{dS}{dt}\right|_{\rm Rad} + T\left.\frac{dS}{dt}\right|_{\rm Conv} = 4\pi\kappa(J-B) + T\left.\frac{dS}{dt}\right|_{\rm Conv}, \quad (2)$$

where T is the temperature, S the entropy per gram, κ the opacity per gram, J the mean intensity and B the integrated Planck function. Here the radiative damping function $\left.\frac{dS}{dt}\right|_{\rm Rad}$ is allowed to vary as function of height and time while the term $T\left.\frac{dS}{dt}\right|_{\rm Conv}$ is time independent and is only a function of the Lagrange height a. This latter function is evaluated at time $t=0$ using Eq. (2) and the requirement that the initial radiative and convective equilibrium atmosphere must not show any time dependence $\left(\left(\frac{\partial S}{\partial t}\right)_a = 0 \text{ at } t=0\right)$.

d) Boundary Conditions

For the hydrodynamic boundary conditions (cf. Ulmschneider et al., 1978) we assume a transmitting boundary at the top of the atmosphere and a piston at the bottom where the velocity is specified by

$$u_1 = -\left(\frac{2F_{M_0}}{\varrho_1 c_1}\right)^{1/2} \sin\left(\frac{2\pi}{P}t\right), \quad (3)$$

where ϱ_1 and c_1 are the density and sound velocity respectively. F_{M_0} is the initial acoustic energy flux and P the period of the acoustic waves. The radiative boundary condition were $I_N^- = 0$ for the ingoing intensity at the top boundary and

$$I_1^+ = \frac{\sigma}{\pi}T_1^4 + \frac{3\mu}{4\pi}F_{\rm Rad} \quad (4)$$

for the outgoing intensity at the bottom boundary where $F_{\rm Rad}$ is the constant radiative flux evaluated from the initial atmosphere, σ the Stefan Boltzmann constant and $\mu = 1/\sqrt{3}$ the angle cosine. In several computations we had numerical difficulties with this radiative boundary condition. In these cases we arbitrarily took $\left(\frac{\partial S}{\partial t}\right)_a = 0$ at the piston boundary. Placing the piston at various optical depths we found that the solution was not noticeably influenced by this procedure.

Table 1 shows the optical depths $\tau_{1/2}$ where the generated acoustic flux has accumulated to one half of its final value. The position of the piston boundary has been chosen according to the following considerations. It should be placed at a height where the acoustic energy flux is generated, where the boundary condition (4) is valid and where the temperature slope is not too steep to avoid excessive computation time when the Courant condition is satisfied for a narrow mesh size. These requirements cannot be satisfied simultaneously. As the acoustic wave initiated by the piston caused considerable perturbations at the lower boundary we found it necessary to place at the piston at optical depths τ_P of between $\tau_{1/2}$ and $3\tau_{1/2}$. The number of points per half wavelength was usually 12 but increased to 15 in cases where radiation damping was important. An extreme example was the model with $T_{\rm eff} = 5000$ K, $\log g = 3$ where we had to take 20 points per half wavelength and $\tau_P = 1500$. The total number of grid points usually was between 120 and 150.

3. Results

a) Temperature Minima, Types of Chromospheres

Table 1 gives the effective temperatures $T_{\rm eff}$ and gravities g of the stellar models selected for this work. Under the assumption of a

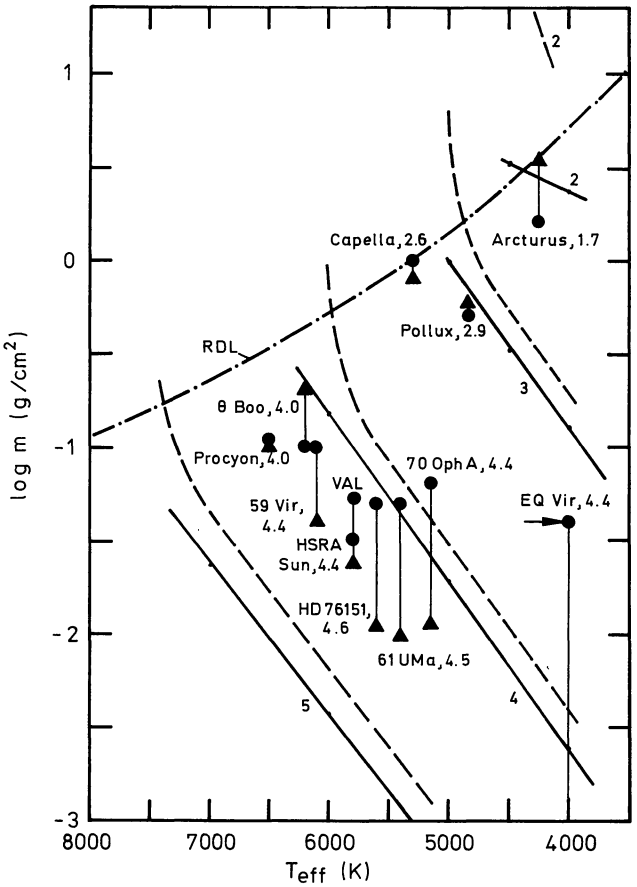

Fig. 2. Mass column densities at the heights of shock formation m_S (dashed) and the theoretical temperature minima m_T (drawn) as function of effective temperature $T_{\rm eff}$. The curve labelled RDL is the radiative damping limit defined in Section 3a. Circles represent empirical and triangles theoretical values, m_E and m_T respectively, for individual stars taken from Papers III and IV. Numbers indicate gravities log$g$. The value m_T of a model with $T_{\rm eff}=4000$ K and log$g=4$ and an initial acoustic flux F_{Mo} increased tenfold is shown by an arrow. The value m_T for EQ Vir is below the lower boundary of the plot

ratio of mixing length and pressure scale height of $\alpha=1.25$ the acoustic flux F_{M_0} and the period P (cf. Table 1) as well as an initial atmosphere model in radiative and convective equilibrium is evaluated as described above. The acoustic wave enters this atmosphere model as soon as the piston at the bottom of the atmosphere is driven according to Eq. (4). After a time of usually ten to twenty periods the time averages over the physical variables become stationary for heights less and including the temperature minimum region. Table 1 and Fig. 2 show the thus obtained mass column densities at the point of shock formation, m_S (dashed), and at the height of the temperature minimum, m_T (drawn). Table 1 contains also the mass column densities of the outer limit of the radiation damping zone, m_L, which are defined as those heights in the initial radiative and convective equilibrium models where the radiative relaxation time (Ulmschneider et al., 1979)

$$t_{\rm Rad}=\frac{2.5c_v}{16\kappa\sigma T^3} \tag{5}$$

is equal to the wave period P given by Eq. (1). Here c_v is the specific heat at constant volume. A very crude extrapolation of the m_L and m_T values of Table 1 allows to construct a line $m_{\rm RDL}(T_{\rm eff})$ in Fig. 2 (labeled RDL) where $m_T(T_{\rm eff})=m_L(T_{\rm eff})$ which we call radiation damping limit. We find approximately

$$m_{\rm RDL}=1.76\,E20\,T_{\rm eff}{}^{-5.43}\,. \tag{6}$$

In Fig. 2 it is seen that the theoretical chromosphere models can be classified into two principal types. For stars with lower $T_{\rm eff}$ and higher gravities the position of the temperature minimum is essentially determined by the height of *shock formation*. We call this type of chromosphere an *S-type chromosphere*. Once formed, the shock grows rapidly in amplitude, leading to quickly rising dissipation and an early formation of a temperature minimum where roughly $m_T\simeq 0.7m_S$. A typical example of an *S*-type chromosphere star is the sun (Ulmschneider et al., 1978). For stars with higher $T_{\rm eff}$ and lower gravities the position of the temperature minimum is mainly determined by *radiation damping*. We call these chromospheres *R-type chromospheres*. In these stars as shown in Table 1 shock formation occurs within the radiative damping zone or close to its upper limit ($m_L\lesssim m_S$). Here strong radiation damping prevents the shock from growing and dissipating. Only after the radiation damping zone has been passed does increasing shock dissipation lead to a temperature minimum ($m_T\lesssim m_L$). Thus in *R*-type chromosphere stars due to radiation damping a large separation exists between the heights of shock formation and of the temperature minimum ($m_T\ll m_S$). A typical example for these kinds of stars is Arcturus (Ulmschneider et al., 1979).

S-type and *R*-type chromospheres are separated in Fig. 2 by a line at $m=0.2m_{\rm RDL}$.

In addition Fig. 2 presents the semi-empirical and the theoretical temperature minimum values m_E and m_T for the stars discussed in Papers III and IV. For cases of Paper III where theoretical values are given only for $\alpha=1.0$ and 1.5, logarithmic interpolations have been plotted. These previous m_T values were computed using the opacity law

$$\kappa=1.376E-23P^{0.738}T^5\ ({\rm cm^2\ g^{-1}})\,. \tag{7}$$

Our present computations however taken the opacity table of Kurucz (1979). For low gas pressure this table gives higher opacities than Eq. (7). Therefore systematic differences exist between the theoretical values of Papers III and IV and the present theoretical results. The temperature slope of the previous theoretical work as seen in Fig. 2 by the values m_T of the stars 70 Oph A, Sun, 59 Vir which all have log$g=4.4$ was less steep than the temperature slope of the present results. This is due to the fact that in later type stars the temperature minima occur in regions of lower pressure. The increased opacity in the present work leads to greater radiation damping which retards the growth of the wave. Shocks are thus formed at greater height and smaller mass column densities.

As can be seen from Fig. 2 as well as from Tables 4 and 5 of Paper III the three stars Arcturus, Capella and Procyon are very close to the radiation damping limit. Because radiative damping is severe in these stars the acoustic waves are strongly weakened and produce temperature minima much below the extrapolated m_T values. We thus expect a significant downturn of the m_T values close to the radiation damping limit which also explains the small temperature slope for the models with log$g=2$.

For a number of models not listed in Table 1 e.g. ($T_{\rm eff}$, log$g$) = (4000 K, 1), (5000 K, 2), (6000 K, 3) and (7000 K, 4) we did not find a theoretical temperature minimum in spite of a

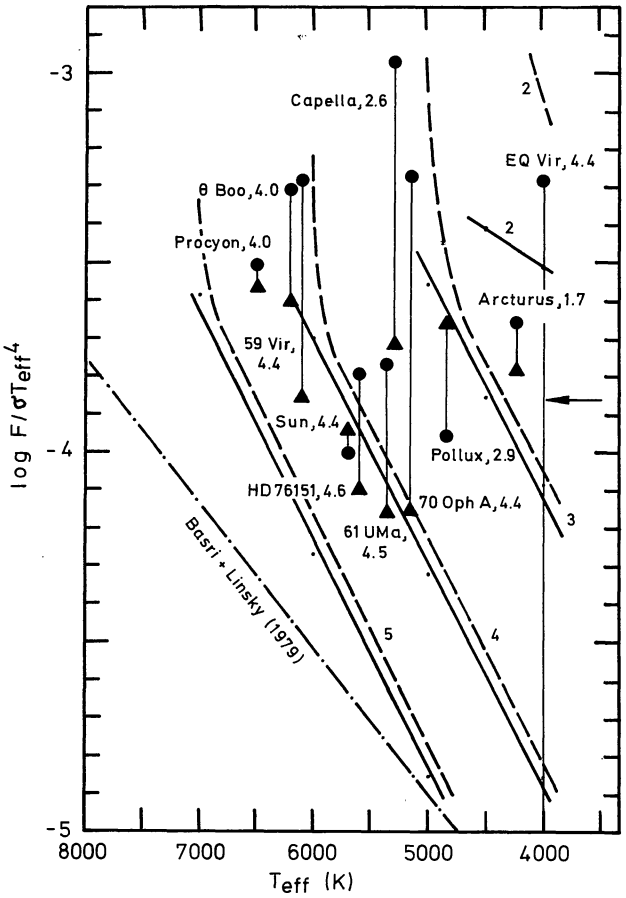

Fig. 3. Acoustic energy fluxes divided by $\sigma T_{\rm eff}^4$ at shock formation F_{MS} (dashed) and at the theoretical temperature minimum F_{MT} (drawn) as function of effective temperature $T_{\rm eff}$. Circles represent semi-empirical chromospheric radiation fluxes F_E and triangles theoretical acoustic fluxes F_{MT} for individual stars taken from Papers III and IV. Numbers indicate gravities log$g$. The flux F_{MT} of a model with $T_{\rm eff}=4000$ K and log$g=4$ and an initial acoustic flux F_{Mo} increased tenfold is shown by an arrow. The average Mg II k_1 radiative flux given by Basri and Linsky (1979) is indicated. The value F_{MT} for EQ Vir is below the lower boundary of the plot

considerable amount of computer time spent to allow for the development of a steady state. The extrapolated m_T values of these stars would lie considerably above the radiation damping limit. This apparently indicates that temperature minima cannot occur deep in a radiative damping zone. The only case where $m_T > m_L$, the model (4500 K, 2), is no exception as here $m_T \simeq m_L$. It should be kept in mind at this point that the term radiation damping limit is not a sharply defined quantity because it only approximately encloses the region where a wave of given period suffers radiation damping.

The values of the mass column density m_T(g/cm^2) of the theoretical temperature minima shown in Fig. 2 and Table 1 can be crudely approximated by the relation

$$m_T = 5.3E-27 T_{\rm eff}^{8.15} g^{-1.36}. \quad (8)$$

Such a steep temperature dependence does not agree well with the observed temperature minima (Cram and Ulmschneider, 1978).

b) Acoustic Fluxes at Shock Formation and the Temperature Minimum

If the dissipation of acoustic shock waves were the principal heating mechanism of stellar chromospheres we would expect that the chromospheric emission fluxes are roughly equal to the acoustic fluxes at the temperature minimum. Figure 3 shows the computed acoustic fluxes F_{MS} at shock formation (dashed) and F_{MT} at the temperature minimum (drawn) together with both theoretical F_{MT} and semi-empirical F_E values from the stars discussed in Papers III and IV. Similar as for the heights of the temperature minima the acoustic fluxes allow to differentiate between two distinct types of theoretical chromospheres. In *S-type chromospheres* where shock formation and temperature minimum essentially coincide we have typically $F_{MT} \simeq 0.8 F_{MS}$ while in *R-type chromospheres* the shocks form in the radiative damping zone which because of $m_T \ll m_S$ leads to $F_{MT} \ll F_{MS}$.

As discussed above for the theoretical temperatures minimum masses the F_{MT} values of the present work likewise are systematically different from those of the previous work. Due to the higher opacity in the present work we have larger radiation damping and consequently smaller fluxes F_{MT} for later type stars relative to the F_{MT} values from Papers III and IV. This can be seen in Fig. 3 by comparing for the three stars 70 Oph A, Sun, 59 Vir which have a common log$g=4.4$ the slope of the F_{MT} values with our present results. As in the case with the temperature minima the acoustic fluxes F_{MT} of the three stars Arcturus, Capella and Procyon do not agree well with the theoretical relations found for the other stars. The reason is the same as mentioned above. Because the temperature minima occur very close to the radiative damping zone limit the acoustic flux F_{MT} suffers a disproportionately large decrease.

c) Temperature Distributions

Figure 4 shows time averaged theoretical temperature distributions for the stellar models listed in Table 1. Also indicated are the radiative and convective equilibrium temperature distributions labelled T_{RE}. As has been noted in earlier work (Ulmschneider et al., 1978; Ulmschneider et al., 1979, Paper III) all models show a temperature depression below the T_{RE} profiles. These depressions arise from the non-linearity of the Planck function when waves of large amplitudes are considered. The distinction of the models in *S*-type and *R*-type chromospheres can also be made on the basis of the temperature profiles. *S-type chromospheres* are characterized by temperature profiles which have first a slowly and later a quickly growing temperature depression. Here the temperature depressions do not become very large and start at relatively small mass close to the temperature minimum. After the temperature minimum there is a rapid temperature rise. In *R-type chromospheres* the temperature depression first grows quickly and later slowly leading to a flat temperature minimum and a slow chromospheric temperature rise. Here the temperature depressions become extensive and start at relatively large mass at great distance from the temperature minimum. A progressively flatter temperature minimum and a decreasing chromospheric temperature gradient in the *R*-type chromosphere stars indicate a continuous transition to the stars of higher $T_{\rm eff}$ and lower gravity above the radiative damping limit where we did not find temperature minima using our present monochromatic approach. It is very instructive to note in Fig. 4 the distinct changes from *R*-type to *S*-type chromospheric temperature distributions, e.g. by going for fixed $T_{\rm eff}=4000$ K from

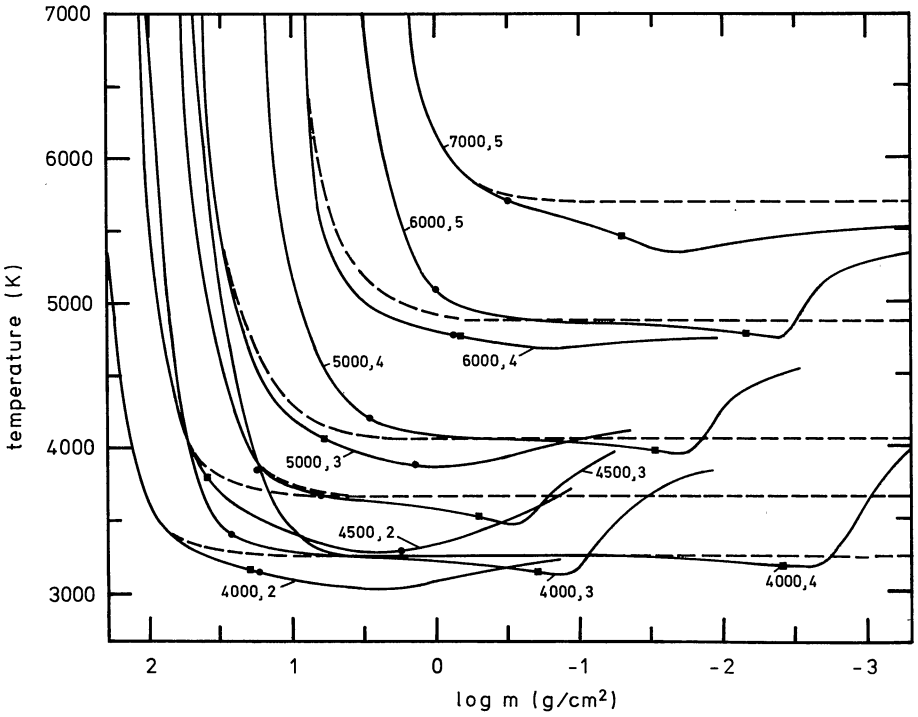

Fig. 4. Theoretical temperature distributions (drawn) as function of the mass column density m for the models listed in Table 1. The models are labeled by the effective temperature $T_{\rm eff}(K)$ and the logarithm of the gravity. Initial grey constant flux atmosphere temperatures are shown dashed. A circle marks for every model the upper limit of the radiative damping zone m_L and a square the shock formation height m_S. In S-type chromospheres the shock formation height occurs close to and in R-type chromospheres at considerable distance from the temperature minimum

lower to higher gravity or by going for fixed gravity $\log g = 4$ from larger to smaller $T_{\rm eff}$.

The different types of temperature distributions can be understood from the way in which temperature minima are generated in the S- and R-type chromospheres. Before the shock forms at heights much greater than the radiation damping limit in S-type chromosphere stars, the wave amplitude and with it the photospheric temperature depression grows rapidly due to energy conservation. Contrary to this and as radiation damping depends on the amplitude, the photospheric temperature depression in R-type chromosphere stars grows less than linearly. Strongly rising shock dissipation leads to the steep chromospheric temperature gradient typical for S-type chromospheres. In R-type chromospheres near the upper limit of the radiative damping zone m_L, shock dissipation is strongly counteracted by radiation damping which continues well past the height m_L. Thus only a gradual chromospheric temperature rise is produced (compare Figs. 2, 6 of Ulmschneider et al., 1978 with Figs. 1, 2 of Ulmschneider et al., 1979). These different types of temperature behaviour are also apparent in the profiles of Paper III (Fig. 1). Note that Pollux as well as our present model $(T_{\rm eff}, \log g) = (7000\,{\rm K}, 5)$ show an intermediate type distribution.

4. Discussion

a) Inadequacies of the Present Version of the Acoustic Heating Theory

Before we compare the predictions of the acoustic heating theory with observations we want to recall the various approximations made in the present version of the theory. As has been discussed above there are three steps in the acoustic heating theory, the construction of a convection zone model, the calculation of the acoustic energy generation and the computation of the propagation and dissipation of the acoustic energy.

The difficulties associated with the mixing length theory are well known (Gough, 1976a, b) and do not need to be repeated here. One of the main shortcomings of the present version of the acoustic heating theory however is the missing acoustic energy for late type dwarf stars. Observations of Blanco et al. (1974) as well as Cram and Ulmschneider (1978) have prompted a search for the reasons of this flux deficite. Preliminary results from this work show that our method to compute the acoustic flux exhibited in Paper I is deficient in several respects. In preliminary calculations Bohn (1980) finds cases in which the acoustic flux is increased by several orders of magnitude. Whether these calculations will suffice however to provide for the missing flux can only be judged when the complete results are available.

Let us now discuss approximations made in the computation of the wave propagation. A basic deficiency of our present theory is the neglect of inhomogeneities of various kinds. The one dimensional method presently used does not allow for the observed spacial inhomogeneity between network and non network regions. As discussed by Linsky (1980) this may be a severe difficulty when we compare our theoretical results with observations because recent empirical models heavily favour network regions. There are other inhomogeneities which have been neglected. Aerodynamic sound generation and propagation actually is a three dimensional phenomenon which occurs at locations that vary statistically in space and time. Obviously we carry great risks when we replace a large number of local phenomena by a one dimensional homogeneous description with a continuous rate of acoustic energy flow. Here we have been guided by the situation usually accepted in stellar atmospheres and have justified the homogeneous approach by the fact that we look at the star globally and average over many structures. However this averaging process is subject to discussion.

Because acoustic flux spectra for stars are presently not available, another type of homogenization has been made by replacing the flux spectra with a delta function at a period located at an estimated flux maximum. Previous work (Ulmschneider and

Kalkofen, 1977; Ulmschneider et al., 1978) has shown that the wave period is a critical parameter for the amount of radiation damping and influences considerably the height of shock formation. Thus it is quite possible that acoustic waves with a statistical range of periods and amplitudes will have significantly different properties relative to monochromatic waves which we presently employ. That changing of frequency components gives a significant effect is seen in the behaviour of the transients at the start of our calculations (cf. Fig. 4 of Ulmschneider et al., 1978).

The grey two stream approximation for the treatment of radiation damping and the assumption of LTE especially for the H^- emission represent stringent restrictions which could however be overcome with a more elaborate code and a significantly increased computation time. Another restriction of our work which could be surmounted in future treatments is the neglect of H and He ionizations and H_2 dissociation. Ionization and recombination time scales in relation to the wave periods would also have to be carefully evaluated in stellar applications. In addition there is a rather difficult problem, possibly not so much for the temperature minimum region but certainly for the higher chromosphere. This is the necessity of a Non-LTE treatment of radiative losses from chromospheric emission lines. This problem could also in principle be solved given enough computer time and core space. However in hydrodynamic calculations in order to arrive at meaningful results the calculation time for a single time step should be reasonably small. Thus progress does not only lie in the realization of what processes should be included in an improved theory, but also in how to find efficient yet fairly accurate approximations to take these processes into account.

Finally a severe shortcoming of our present theory could be the neglect of magnetohydrodynamic effects. Different views about the importance of such a treatment have been discussed by Ulmschneider (1979) and Linsky (1980). Except for highly idealized cases as e.g. the computations along vertical magnetic flux tubes (Foukal and Smart, 1980) such treatments would be very complicated as they essentially involve two dimensional geometries. For this purpose typical magnetic field configurations not only for the sun but for a large number of other late type stars would have to be known. Aside of the enormously increased computation time we did not attempt a magnetohydrodynamic treatment because of two reasons. Firstly we think it unwise to attempt a magnetohydrodynamic treatment before the acoustic approach is fully explored and secondly we hope to learn most by comparing the observations with a theory that has a minimum of degrees of freedom.

b) *The Prediction of Temperature Minima*

Let us now discuss the ability of the acoustic heating theory to predict temperature minima. Because of the numerous approximations made in the present version of this theory we expect rather large errors. In a comparison with observations these errors are magnified by the observational uncertainties of the semi-empirically obtained temperature minima derived almost exclusively from Mg II and Ca II line data. In spite of these uncertainties Fig. 2 shows a rather good agreement between the theoretical and semi-empirical mass column densities, m_T and m_E, at the temperature minima. This agreement however deteriorates towards late type dwarf stars.

Especially the gravity dependence of the observations seems to be nicely reproduced. Assuming that the empirical relation $m_E(T_{\rm eff})$ between mass and $T_{\rm eff}$ at constant gravity $\log g \simeq 4.4$ is roughly determined by the five stars 70 Oph A, 61 UMa, Sun (VAL), 59 Vir and EQ Vir and using the value $m_E = 1.8\,{\rm g/cm^2}$ for Arcturus we find the relation

$$m_E = 1.5{\rm E}-9\, T_{\rm eff}^{2.8} g^{-0.66}\,. \tag{9}$$

Note that a similar empirical relation given by Cram and Ulmschneider (1978, Fig. 1) has an even smaller gravity dependence which is probably due to the connection between m_E and the width $\Delta\lambda_1$ adopted by these authors. Nevertheless Eq. (9) has a much smaller gravity dependence than found in our theoretical results as given by Eq. (8). This appears to be mainly due to the steep $T_{\rm eff}$ dependence of our theoretical results which is caused by missing acoustic flux for late type dwarf stars. As preliminary work by Bohn (1980) indicates that an improved method of the acoustic energy generation results in a considerably enhanced acoustic flux we have computed a model of $T_{\rm eff} = 4000\,{\rm K}$ and $\log g = 4$ with a factor of ten more acoustic energy. The resulting temperature minimum mass m_T is indicated by an arrow in Fig. 2. Connecting this value m_T with unmodified m_T values at the same gravity but higher $T_{\rm eff}$ we almost reproduce the observed temperature and gravity dependences.

Discrepancies with observed temperature minima arise for the stars above the radiative damping limit (cf. Fig. 2 and Sect. 3a) where we did not find temperature minima. As summarized by Ulmschneider (1979) chromospheres and consequently temperature minima are observed in all stars except possibly *A* stars. We attribute these missing temperature minima to our grey, Rosseland, LTE radiation treatment and to the use of a monochromatic acoustic wave. An acoustic flux spectrum would obviously lead to a not so sharply defined radiation damping limit which very strongly depends on the adopted wave period.

Finally as already noted in Paper III important corrections to the theoretical positions of the temperature minimum masses m_T are expected if a nongrey treatment of the radiation transport were made. For the sun work based on non grey ambient models (Paper II) showed better agreement between theoretical and empirical temperature minimum positions.

c) *Temperature Distributions and Type of Chromospheres*

In Sect. 3 we have found that the theoretical chromosphere models fall into two distinct classes, the *S-type chromospheres* where the temperature minimum is closely correlated with the height of shock formation and the *R-type chromospheres* where the temperature minimum is essentially determined by radiation damping. Can this classification be seen in the semi-empirical models? We compare our results with the empirical temperature profiles for Capella and Pollux (Kelch et al., 1978), 70 Oph A (Kelch, 1978) and θ Boo, 59 Vir, HD 76151, 61 UMa, EQ Vir (Kelch et al., 1979). At the first glance our theoretical temperature distributions appear to be quite different from the empirical profiles. In the photosphere the empirical models not only show a much steeper temperature profile but they have a temperature *enhancement* while our models show a temperature *depression*.

Let us first discuss the photospheric temperature slope. If we remove the modifications due to the chromosphere in the empirical models as well as the effects of the acoustic waves in the theoretical models then the differences in the remaining temperature slopes would simply be those between nongrey and grey constant flux atmospheres. This shows that here the theoretical models suffer from the grey approximation and that a nongrey treatment would largely remove this discrepancy. This has already

been noted earlier (Ulmschneider et al., 1978). A rough estimate of the effect of such a nongrey treatment on the theoretical models can be made by adding the theoretical temperature depressions below the T_{RE} profiles in Fig. 4 to the nongrey constant flux profiles.

The second apparent discrepancy between the theoretical and the empirical photospheric temperature distributions is that the theoretical profiles show a temperature depression while the empirical profiles have a temperature enhancement. This disparity in our view can be explained by the large amplitude and by the shape of the acoustic waves (see also Ulmschneider et al., 1978). In the absence of mechanical heating in the layers below the temperature minimum the temperature depression arises from the fact that radiative equilibrium [cf. Eq. (2)] has to be satisfied in the time mean. While the mean intensity J in the outer layers of a star is essentially constant, the Planck function B due to the T^4 dependence causes a disproportionately larger emission at the wave crest that at the wave trough. Consequently to satisfy radiative equilibrium in the time mean the temperature must oscillate around a mean value which is lower than T_{RE}. This temperature depression however is not "observed" at optical wavelengths because the enhanced emission by the wave, due to the usual assumption of a smooth temperature distribution, is attributed to a correspondingly higher mean temperature. Here optical wavelengths refer to those parts of the spectrum where the main radiative energy transport occurs in those photospheric layers. The semi-empirical models are based on the Mg II h and k as well as on the Ca II K line observations. At the corresponding Planck function has an even greater temperature dependence than at the optical wavelengths where the photospheric radiation flux is emitted. We thus expect that the same process which causes the temperature depression to ensure energy balance at optical wavelengths *must leat to enhanced emission in the* UV which is observed as an apparent temperature enhancement. This effect which has been suggested to us by Kalkofen (1979) may also explain the temperature difference between the empirical solar chromosphere models based on the Mg II lines and those based on Ca II K line observations (Linsky and Ayres, 1978, Fig. 1; see also Avrett, 1977, as well as Wilson and Williams, 1972).

Because the temperature depression and the temperature enhancement both depend on the same process the temperature enhancement must have roughly the same height variation as the temperature depression. Is this borne out by the observations and can the differentiation between S- and R-type chromospheres be seen in the empirical data? We indeed believe that the behaviour of the S- and R-type chromospheres is found in the observations. In θ Boo and Capella the large temperature enhancements start at comparatively large mass column densities growing first rapidly and later slowly similar to the temperature depressions in the R-type chromospheres. That θ Boo has an R-type theoretical chromosphere is seen from Table 1 of Paper IV where $m_S \gg m_T$. As opposed to θ Boo and Capella the stars 59 Vir, HD 76151, 61 UMa, Eq Vir and 70 Oph A exhibit a temperature enhancement which starts at low mass column density comparatively close to the temperature minimum, has a linear growth and reaches only small magnitude, similar to the temperature depressions in S-type chromospheres. Pollux in agreement with out theoretical results appears to have an intermediate type chromosphere. In addition to the fact that the differentiation into R- and S-type chromospheres can be seen in the temperature distributions of individual stars it should be noted that this behaviour also correlates well with the position in the HR diagram. It is seen in Fig. 2 that Capella and θ Boo both are in the region close to the radiation damping limit where R-type chromospheres occur while 59 Vir, HD 76151, 61 UMa, EQ Vir and 70 Oph A all fall into the region where S-type chromospheres are expected.

Let us finally discuss the chromospheric temperature rise. As noted by Ulmschneider et al. (1978) the theoretical chromospheric temperature rise produced by the present method is not very realistic as we have neglected the departure from LTE of the most important chromospheric emitters H^-, Mg II and Ca II. In Fig. 4 e.g. for the models with $T_{\rm eff} = 4000$ K we see that the theoretical chromospheric temperature gradient increases with increasing gravity going from R-type to extreme S-type chromospheres. A similar steepening is seen in Fig. 4 if for the models with $\log g = 4.0$ we go from high to low $T_{\rm eff}$. Although not as pronounced the empirical temperature distributions show a similar trend. The chromospheric temperature gradients of θ Boo and Capella are much smaller than e.g. those of EQ Vir and 70 Oph A.

d) Comparison with Radiation Loss Rates from Empirical Chromosphere Models

If the acoustic heating theory were the principal heating mechanism of the chromosphere then as the main radiation loss (cf. Ulmschneider, 1979, Table 1) occurs in the lower chromosphere the acoustic flux at the temperature minimum should be roughly equal to the total chromospheric radiation loss. Not insisting on complete equality we allow for a possible additional heating mechanism for the upper chromosphere. In Fig. 3 for a number of individual stars we have plotted empirical chromospheric loss rates F_E computed from semi-empirical chromospheric models. These values were taken from Papers III and IV.

The comparison of the F_E values with acoustic fluxes F_{MT} at the temperature minima shows considerable discrepancies. This is expected. As pointed out by Linsky (1980) the empirical chromospheric models being constructed from Mg II and Ca II line observations are not very suitable for the calculation of the dominant H^- losses. These line-based empirical models do not heavily favour plage regions but may be considerably hotter than continuum models as has been shown for the sun (Avrett, 1977; Linsky and Ayres, 1978). In addition the method to compute the H^- losses is still debated (cf. Praderie and Thomas, 1976; Kalkofen and Ulmschneider, 1979). Furthermore the F_{MT} values are also not free of considerable errors. Radiation damping in our theoretical computations is rather crudely treated by a grey two stream approximation and by neglecting non-LTE effects in H^-. Thus considerable error bars have to be present in a comparison between the fluxes F_{MT} and F_E. If we assume an error of roughly a factor of six (cf. Paper III) there seems to be a reasonable agreement (see Fig. 3) except for the three stars Capella, 70 Oph A and EQ Vir. Capella belongs to the RS CVn type variables for which Basri and Linsky (1979) find unusually large Mg II emission which they attribute to a magnetic heating mechanism. However it should be noted that Capella is an R-type chromosphere star (see Fig. 2) which lies very close to the radiative damping limit. As radiative damping is severe for this star and in view of our grey LTE approach, we expect particularly large errors in the theoretical fluxes F_{MT}. Moreover the empirical model of Capella exhibits a large temperature enhancement which after the discussion in Sect. 4c indicates that such a model is especially bad for the computation of the H^- loss F_E.

For the stars 70 Oph A and EQ Vir (cf. Papers III, IV) we again find the acoustic flux deficite for late type stars. Enhancing the initial acoustic flux by a factor of ten in a model with $T_{\rm eff} = 4000$ K

and $\log g = 4$ we find a ten times higher acoustic flux at the temperature minimum. This is indicated by an arrow in Fig. 3. It could however also be that for stars like EQ Vir a magnetic heating mechanism or acoustic energy enhancement due to magnetic fields augments the acoustic energy flux.

e) Comparison with Observed Chromospheric Radiation Losses

In his review article on stellar chromospheres Linsky (1980) suggested two additional tests to compare theoretical computations with observations. He proposed that theoretical chromosphere models should correctly predict the $T_{\rm eff}$ and gravity dependences of the observed chromospheric radiation loss rates and that they should show the observed scatter in the Mg II and Ca II emission rates in stars of identical $T_{\rm eff}$ and gravity.

From the main chromospheric emitters (cf. Ulmschneider, 1979, Table 1) the dominant H^- losses cannot be observed directly because of the luminous H^- emission of the photosphere. The Ca II H and K lines are also not ideal observables desired for a direct comparison because of the necessary subtraction process of the photospheric emission. Only for the Mg II h and k lines is the photospheric background weak enough that these lines provide the desired directly observable chromospheric parameters against which the $T_{\rm eff}$ and gravity dependences of our acoustic fluxes can be tested.

In the lower portion of Fig. 3 we have plotted the mean observed Mg II k_1 line flux averaged over many stars as given by Basri and Linsky (1979, Fig. 3). The temperature slope of this relation agrees rather well with out theoretical results. Figure 3 shows that the averages of both the theoretical acoustic fluxes F_{MT} and the semi-empirical radiation fluxes F_E for the stars taken from Papers III and IV lie higher by roughly a factor of 10 and 12 respectively. It is interesting that after Ulmschneider (1979, Table 1) for the sun the Mg II k_1 line loss is 5.0 E5 erg/cm^2 s while the total chromospheric loss is 6.2 E6 erg/cm^2 s. The flux ratio thus gives just the correct ratio of around 12 demanded for an agreement of the Mg II line observations with both the calculated empirical as well as theoretical chromospheric losses.

However the observations of Basri and Linsky (1979) as well as of Weiler and Oegerle (1979) do not show any gravity dependence. In our previous work (Papers III and IV) we have found that the acoustic flux F_{MT} changes by a factor of roughly four if $\log g$ is decreased from four to two. This is a much smaller gravity dependence than that of the acoustic flux at shock formation F_{MS} given in Paper II. Yet in our present results because of the use of the opacity table of Kurucz (1979) the increased radiation damping leads to an increased gravity dependence of F_{MT} as seen in Fig. 3. This is not inconsistent. If much more acoustic energy in late type dwarf stars were available as is indicated by preliminary work then the masscolumn densities m_T would increase and with it the values F_{MT} for these stars leading to a much decreased temperature slope of the F_{MT} values in Fig. 3. With additional acoustic energy for late type stars we would thus have a temperature slope in agreement with the observations of Basri and Linsky (1979). However it is unlikely that the gravity dependence would vanish completely.

Why can this gravity dependence not be seen in the observations? One possibility in the framework of our present version of the acoustic heating theory is that for stars where the temperature minima approach the radiative damping limit there are similar acoustic fluxes F_{MT} for different stars. This is clearly seen both in Figs. 2 and 3 where e.g. the values m_T and F_{MT} of stars with *R*-type chromospheres like Arcturus, Capella and Procyon are much depressed into regions where stars with *S*-type chromospheres would have similar mass column densities and fluxes. The zone where this overlap occurs however is restricted to the region close to the radiative damping limit where the *R*-type chromospheres occur. Yet if a realistic model were computed taking the full acoustic frequency spectrum into account we possibly might have a much extended multivalued F_{MT} region. Another more likely possibility is that a superposed scatter drowns the gravity dependence in Fig. 3. The possible origin of this scatter is discussed below.

f) Comparison with the Observed Emission Scatter

The acoustic heating theory in its present form depends only on three parameters $T_{\rm eff}$, $\log g$ and the ratio α of mixing length to pressure scale height. Here α is not really a free parameter but indicates our uncertainty in the description of a stellar convection zone. We take $\alpha = 1.25$. With a given and $T_{\rm eff}$ as well as $\log g$ specified for a particular star we thus do not have any freedom of choice left in our theoretical computations. The acoustic heating theory in its present form for a particular star will thus give unambiguous values both for m_T and F_{MT}.

However Linsky and Ayres (1978) as well as Basri and Linsky (1979) find that there are stars with similar values of $T_{\rm eff}$ and $\log g$ but with different Mg II k_1 line fluxes. How is it possible to explain this scatter in the Mg II line fluxes? Linsky (1980) concludes that the acoustic heating theory "*cannot* explain the large diversity of chromospheric radiative loss rates among single stars of similar $T_{\rm eff}$ and gravity". He supposes a *magnetic heating mechanism* and argues that "the correlation of Ca II strength with the magnetic field must be viewed as circumstantial evidence for a hydromagnetic origin of chromospheric heating".

In a general sense we agree with Linsky's conclusions that the observed emission scatter for stars has to do with the presence of magnetic fields much as is observed on the sun. The scatter could be due to the different coverage of a star by plage regions (Basri and Linsky, 1979). The age of the star thus enters the picture with the well known age-rotation – magnetic field correlation (Skumanich, 1972). The large Mg II k_1 emission in RS CVn binaries are then explained as orbital motion converted into rotation which enhances magnetic fields even in old stars (Basri and Linsky, 1979). However the question is whether this magnetic heating candidate is a completely different mechanism as the quasi-steady processes discussed by Ulmschneider (1979, Chapt. 4) or whether the presence of magnetic fields is only the cause of a different behaviour of the acoustic mechanism. We think it premature to presently decide this question.

It is true that the present version of the acoustic heating theory does not explain the scatter associated with the magnetic fields. But an improved (magneto-)acoustic heating theory about which preliminary work already exists (Kulsrud, 1955; Uchida, 1963; Foukal and Smart, 1980) may well be satisfactory. The presence of magnetic flux tubes acts similar to a material boundary and could well allow for dipole sound generation which is much more efficient than the relatively inefficient quadrupole sound generation which we presently employ. Kulsrud (1955) moreover discusses quadrupole sound generation by isotropic turbulence in the presence both of turbulent and of constant magnetic fields. In some cases he finds an enhancement of the acoustic flux by a factor of ten. This could change F_{MT} by a factor of up to ten depending on the relative area of the magnetic regions. Incidentally the scatter seen in Mg II k_1 observations by Basri and Linsky (1979, Fig. 3) also amounts to a factor of ten.

In summary we think that it may well be that the scatter of the Mg II k_1 observations is caused by a presently unknown *magnetic mechanism* especially as the Mg II k_1 observations pertain to the middle and upper chromosphere where magnetic fields become prominent. The acoustic heating theory would then the responsible only for the temperature minimum area. This hypothesis would most naturally explain the large chromospheric radiation losses of EQ Vir and the RS CVn variables HR 1099 and UX Ari (Basri and Linsky, 1979). However we think it even more likely that the scatter is due to enhancement of the acoustic energy generation in the presence of magnetic fields as well as to the influence of magnetic components in the acoustic wave propagation (magneto-acoustic waves).

5. Conclusions

In the present version of the acoustic heating theory the acoustic energy generation is computed using the Lighthill-Proudman theory and convection zone models which employ the Böhm-Vitense theory. The acoustic wave propagation is calculated taking a monochromatic wave and using a grey LTE radiation hydrodynamic code. In spite of the many shortcomings of this approach which have been discussed above (Sect. 4a) we find a *rather good agreement between predictions from our theoretical chromosphere models and empirical chromospheric parameters.* Because of the fact that our theoretical approach does not have any freedom of choice or free parameter left which could be adjusted to minimize discrepancies with observations we have to attach to these agreements even greater importance. We now list the main results.

a) The theoretical and empirical mass column densities at the temperature minima agree rather well except for late type dwarf stars.

b) No temperature minima are found in models of high $T_{\rm eff}$ and low gravity considerably above the radiation damping limit (see Fig. 2). This very likely is due to our approximate treatment of the acoustic spectrum.

c) The theoretical chromosphere models can be differentiated into two classes, *S-type chromospheres* where the temperature minima are closely correlated with the height of shock formation and *R-type chromospheres* where the temperature minima are determined by radiation damping. The *S*- and *R*-type chromospheres have characteristic temperature distributions.

d) It is proposed that the temperature enhancements in empirical chromosphere models like the temperature depressions in the theoretical models both arise from the large amplitude and the shape of the acoustic waves. Large temperature enhancements correlate well with *R*-type and small enhancements with *S*-type chromospheres.

e) Except for late type dwarf stars do we have a fairly good agreement between the acoustic flux at the temperature minimum and the semi-empirical total chromospheric radiation fluxes computed on basis of empirical models. Here Capella is possibly an exception where the strong chromospheric emission may be connected with its RS CVn binary nature and the action of an additional magnetic heating mechanism or acoustic energy enhancement due to magnetic fields.

f) Except for late type dwarf stars do the average Mg II k_1 radiation flux observations of Basri and Linsky (1979) scale well both with the magnitude and the temperature slope of our acoustic fluxes at the temperature minimum.

g) Preliminary work by Bohn (1980) indicates for late type dwarf stars considerable acoustic energy enhancements that we have the hope that much of the above mentioned discrepancy for these types of stars will vanish.

h) Our present calculations do not explain firstly the observed scatter in the Mg II k_1 radiation flux observations and secondly the observed occurence of chromospheres in stars of high $T_{\rm eff}$ and low gravity above the radiative damping limit. Here as discussed above the acoustic theory clearly needs improvements for example by considering enhancement of acoustic energy generation in magnetic field regions and by the detailed incorporation of the acoustic frequency spectrum. Further errors arise from the grey approach, the LTE treatment and the neglect of ionization as well as molecular dissociation. Only if these improvements have been made do we think it advisable to look deeply into a radically different heating mechanism.

Acknowledgement. We would like to thank H. U. Bohn of our institute for many discussions on acoustic energy generation and for permission to quote preliminary results. This work as well as previous work of this series has been made possible by generous support from the Deutsche Forschungsgemeinschaft which we gratefully acknowledge.

References

Avrett, E.H.: 1977, in *The solar output and its variation*, O. R. White (ed.), Colorado Assoc. Univ. Press, Boulder, Col. p. 327
Basri, G.S., Linsky, J.L.: 1979, *Astrophys. J.* **234**, 1023
Biermann, L.: 1946, *Naturwiss.* **33**, 118
Blanco, C., Catalano, S., Marilli, E., Rodono, M.: 1974, *Astron. Astrophys.* **33**, 257
Böhm-Vitense, E.: 1958, *Z. Astrophys.* **46**, 108
Bohn, H.U.: 1980, *Astron. Astrophys.* (in preparation)
Carbon, D.F., Gingerich, O.: 1969, Proc. 3rd Harvard Conf. on Stellar Atmospheres, MIT Press, Cambridge, Mass.
Christensen-Dalsgaard, J., Gough, D.O., Morgan, J.G.: 1979, *Astron. Astrophys.* **73**, 121
Claverie, A., Isaak, G.R., McLeod, C.P., van der Raay, H.B., Roca Cortes, T.: 1979, *Nature* **282**, 591
Cram, L.E., Ulmschneider, P.: 1978, *Astron. Astrophys.* **62**, 239
Foukal, P., Smart, M.: 1980, *Solar Phys.* (to be published)
Gough, D.: 1976a, *Proc.* IAU *Coll.* **38**, Problems of stellar convection, E.A. Spiegel, J.P. Zahn Eds., p. 15
Gough, D.: 1976b, *Proc.* IAU *Coll.* **36**, The energy balance and hydrodynamics of the solar chromosphere and corona, R. M. Bonnet, Ph. Delache Eds., p. 3
Iben, I., Jr., Mahaffy, J.: 1976, *Astrophys. J.* **209**, L39
Kalkofen, W.: 1979 (private communication)
Kalkofen, W., Ulmschneider, P.: 1977, *Astron. Astrophys.* **57**, 193
Kalkofen, W., Ulmschneider, P.: 1979, *Astrophys. J.* **227**, 655
Kelch, W.L.: 1978, *Astrophys. J.* **222**, 931
Kelch, W.L., Linsky, J.L., Basri, G.S., Chiu, H.Y., Chang, S.H., Maran, S.P., Furenlid, I.: 1978, *Astrophys. J.* **220**, 962
Kelch, W.L., Linsky, J.L., Worden, S.P.: 1979, *Astrophys. J.* **229**, 700
Kulsrud, R.M.: 1955, *Astrophys. J.* **121**, 461
Kurucz, R.: 1973, Memo to ATLAS users, SAO Spec. Rept. 309
Kurucz, R.: 1979, *Astrophys. J. Suppl.* **40**, 1
Lighthill, M.J.: 1952, *Proc. Roy Soc. London* A**211**, 564
Lighthill, M.J.: 1954, *Proc. Roy Soc. London* A**222**, 1
Linsky, J.L., Ayres, T.R.: 1978, *Astrophys. J.* **220**, 619
Linsky, J.L.: 1980, *Proc.* IAU *Coll.* **51**, Turbulence in Stellar Atmospheres, (in press)
Praderie, F., Thomas, R.N.: 1976, *Solar Phys.* **50**, 333

Proudman, I.: 1952, *Proc. Roy Soc. London* A**214**, 119
Renzini, A., Cacciari, C., Ulmschneider, P., Schmitz, F.: 1977, *Astron. Astrophys.* **61**, 39
Rhodes, E.J., Jr., Ulrich, R.K., Simon, G.W.: 1977, *Astrophys. J.* **218**, 901
Schmitz, F., Ulmschneider, P.: 1980a, *Astron. Astrophys.* **84**, 191
Schmitz, F., Ulmschneider, P.: 1980b, *Astron. Astrophys.* **84**, 93
Skumanich, A.: 1972, *Astrophys. J.* **171**, 565
Stein, R.F.: 1968, *Astrophys. J.* **154**, 297
Stein, R.F.: 1970, private communication
Uchida, Y.: 1963, *Publ. Astron. Soc. Japan* **15**, 376
Ulmschneider, P.: 1979, *Space Sci. Rev.* **24**, 71
Ulmschneider, P., Kalkofen, W.: 1977, *Astron. Astrophys.* **57**, 199
Ulmschneider, P., Kalkofen, W., Nowak, T., Bohn, U.: 1977a, *Astron. Astrophys.* **54**, 61
Ulmschneider, P., Schmitz, F., Hammer, R.: 1979, *Astron. Astrophys.* **74**, 229
Ulmschneider, P., Schmitz, F., Kalkofen, W., Bohn, H.U.: 1978, *Astron. Astrophys.* **70**, 487
Ulmschneider, P., Schmitz, F., Renzini, A., Cacciari, C., Kalkofen, W., Kurucz, R.: 1977b, *Astron. Astrophys.* **61**, 515
Ulrich, R.K., Rhodes, E.J., Jr.: 1977, *Astrophys. J.* **218**, 521
Weiler, E.J., Oegerle, W.R.: 1979, *Astrophys. J. Suppl.* **39**, 537
Wilson, P.R., Williams, N.V.: 1972, *Solar Phys.* **26**, 30